

## Delay of a microwave pulse in a photonic crystal

V. S. Babitski,<sup>1</sup> V. G. Baryshevsky,<sup>2</sup> A. A. Gurinovich,<sup>2</sup> E. A. Gurnevich,<sup>2</sup> P. V. Molchanov,<sup>2</sup> L. V. Simonchik,<sup>1</sup> M. S. Usachonak,<sup>1,a)</sup> and R. F. Zuyewski<sup>3</sup>

<sup>1</sup>*Institute of Physics of NAS of Belarus, 68 Nezavisimosti Ave., 220072 Minsk, Belarus*

<sup>2</sup>*Institute for Nuclear Problems, Belarusian State University, 220030 Minsk, Belarus*

<sup>3</sup>*Museo Storico della Fisica e Centro di Studi e Ricerche "Enrico Fermi," Piazza del Viminale, 1, 00184 Roma, Italy and CERN, CH-1211 Geneva 23, Switzerland*

(Received 16 May 2017; accepted 14 August 2017; published online 28 August 2017)

Propagation of a nanosecond microwave pulse through a photonic crystal placed into an X-band waveguide is investigated. The nanosecond pulse is produced via shortening of the microsecond microwave pulse by the plasma electromagnetic band gap structure, which is formed in the waveguide by microwave breakdown ignited discharges inside three neon-filled glass tubes. Measured delay time for nanosecond microwave pulse propagation through the photonic crystal is about 23 ns that is in good agreement with the value obtained by numerical simulation. This time delay value corresponds to the group velocity of microwave pulses in the photonic crystal  $v_{gr} \approx 0.11c$ , where  $c$  is the speed of light in vacuum. *Published by AIP Publishing.*

[<http://dx.doi.org/10.1063/1.5000239>]

### I. INTRODUCTION

There has been increasing interest in electromagnetic pulses propagating in matter with the group velocity much smaller than the speed of light in vacuum in recent decades. Multiple studies report significant reduction of group velocity  $v_{gr}$  of an X-ray pulse passing through a crystal, when Bragg diffraction of X-ray photons in crystals occurs. Such slowing down is caused by strong dispersion of the medium refraction index in the vicinity of Bragg conditions for the incident radiation.<sup>1,2</sup> The utility of short pulse X-ray diffraction in a variety of different applications has been already proven. Time-dependent X-ray diffraction is of great interest for both theoretical<sup>3–6</sup> and experimental<sup>7</sup> studies. Implications of X-ray pulse shaping for XFEL applications can be clearly addressed:<sup>8</sup> crystal optics components of X-ray FELs enable reduction of intensity fluctuations or increase of monochromaticity of the radiated beam.

The effect of group velocity reduction for a wave in a spatially periodic matter exists for different ranges and a variety of waves due to generality of laws of wave diffraction. Thus, neutron delay in crystals in conditions of diffraction was predicted and observed.<sup>9</sup>

Slow light, which is a promising solution for time-domain processing of optical signals, is a subject of multiple studies.<sup>2,10–12</sup> Particularly, measurements of group velocity and optic pulse delay in photonic crystals were carried out<sup>13–15</sup> to ground application of photonic crystals as true time delay lines,<sup>13</sup> slow-light enhanced optical modulators,<sup>14</sup> etc. Optical elements for laser pulse shaping are widely studied to be applied for fast optical information processing, analog optical computing, laser material processing, and coherent control.<sup>16–18</sup>

To verify performance of guided-wave photonic devices with a high-index contrast in the microwave range the

experimental method<sup>19</sup> was introduced. In particular, the authors designed the photonic crystal waveguide as an air-bridge structure with a slab permittivity of  $\epsilon_r = 10$  and a total length of about 30 cm and demonstrated that at the pass band edge of this waveguide near 10.5 GHz the pulse group velocity was 4%–20% of the speed of light.

The effect of pulse delay also reveals for radiation generated by an electron beam in a spatially periodic matter (natural crystal, photonic crystal,<sup>20</sup> etc.) in all spectral ranges (X-ray, optical, THz, and microwave).<sup>20–23</sup> Experimental observation of this effect for microwave radiation generated by an electron beam in the photonic crystal built of metal threads was reported in Ref. 21.

In the present paper, the experiment to observe and measure the microwave pulse delay in the specially designed photonic crystal (spatially periodic structure built of metal rods inside the X-band waveguide) is described. Measured time delay is compared with that obtained by numerical simulation.

### II. APPROACH

The microwave pulse, whose propagation in the photonic crystal is studied, has the central frequency 9.15 GHz and the field structure corresponding to the  $TE_{10}$  mode of a rectangular waveguide. The photonic crystal [see Fig. 1(a)] is designed as a spatially periodic structure built of copper rods inside a WR90/R100 waveguide of 1 m length. Each crystal plane comprises 3 copper rods of 1.25 mm diameter placed normally to the wider waveguide wall and distributed symmetrically to the central rod at the distance  $L = 7.7$  mm from each other and  $L/2$  from the waveguide side wall. The crystal period  $d = 23.2$  mm provides the upper edge of the transmission band to be in the vicinity of 9.15 GHz [Fig. 1(b)], thus making the group velocity for the radiation pulse of this frequency propagating in the photonic crystal to be much smaller as compared to the speed of light in vacuum.

<sup>a)</sup>E-mail: m.usachonak@dragon.bas-net.by

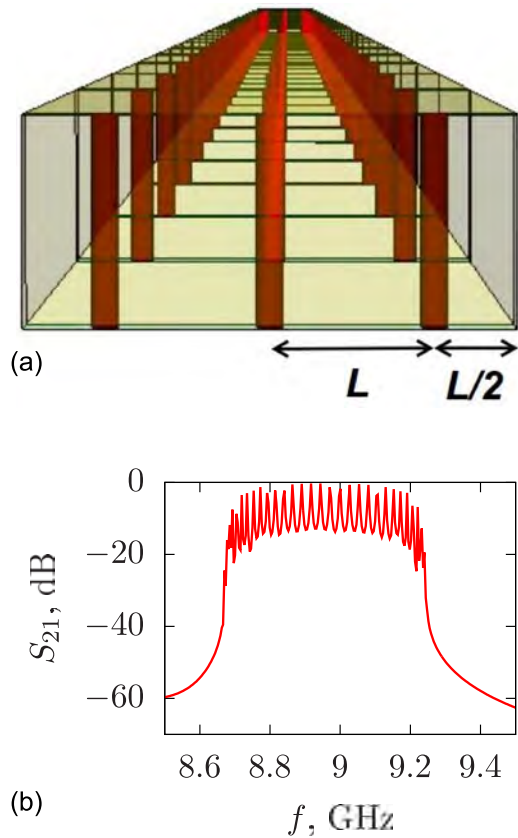


FIG. 1. 3D model of the photonic crystal (a) and calculated pass band (b).

Frequency response [Fig. 1(b)] shows some amplitude ripples, whose number is determined by the number of crystal periods.

### A. Simulation

Microwave pulse propagation in the photonic crystal was simulated by CST Microwave Studio<sup>24</sup> with the goal to define the incident pulse duration making pulse delay effect evident. The delay time is proportional to the number of periods of the photonic crystal (crystal length  $L_{cr}$ ), which for both simulation and experiment was equal to 33. Here, the incident pulse duration means duration at  $-3$  dB level of maximal pulse amplitude.

Simulated intensity of the pulses transmitted through the photonic crystal for the incident pulses of different durations (30, 10, and 5 ns) is shown in Fig. 2. Time zero corresponds to the maximum of incident wave intensity. The delay effect is well resolved, when the duration of the incident pulse is 10 ns and shorter. In this case, the intensity oscillations, which are caused by Bragg diffraction of the incident wave in the photonic crystal, are well distinguished. When the pulse duration is equal to or exceeds the delay time  $\tau = L_{cr}/v_{gr}$ , these oscillations appear flat (see the transmitted pulse shape for 30 ns incident pulse duration in Fig. 2).

To illustrate the ratio of incident, transmitted, and reflected wave amplitudes, they three are shown in Fig. 3 for the incident pulse of 4 ns duration. The reflected pulse amplitude is comparable with that of the incident pulse and the time delay between incident and reflected pulses is about

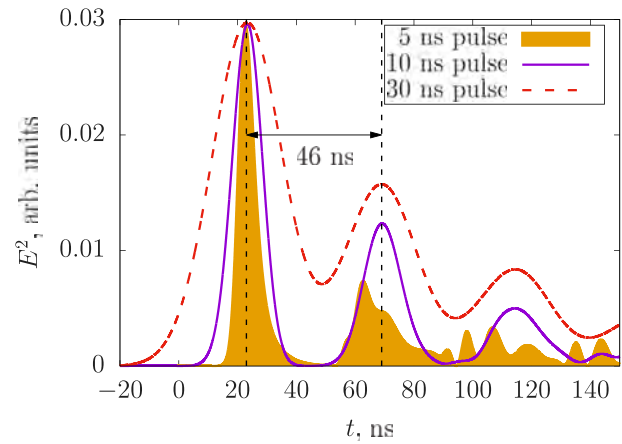


FIG. 2. Simulated intensity of the pulses transmitted through the photonic crystal for the incident pulses of different widths (5, 10, and 30 ns). The delay time is about 23 ns.

2 ns. The amplitude of the transmitted signal is much smaller than that of the incident pulse, the transmitted pulse delay (time between maxima of incident and transmitted pulses) is about 23 ns and both the transmitted and reflected pulses have a chain of equidistant peaks with the time interval between adjacent those of about  $2\tau$ .

### B. Experimental setup

The experimental layout and the setup photo are presented in Fig. 4. Specially designed magnetron is used as a pulsed microwave source, whose key parameters are as follows: frequency about 9.15 GHz, pulse duration about 150 ns, repetition rate about 2 kHz, and peak power about 50 kW.

Microwave pulse shortening is produced by a plasma electromagnetic band gap (EBG) structure (or electromagnetic crystal)<sup>25</sup> formed in a WR90/R100 waveguide section by low pressure discharges in three sealed-off glass tubes. In the experiment, the commercial gas-discharge noise diodes “GSh-6,” whose inner and outer diameters are 1.6 mm and 2.2 mm, respectively, are used. Tubes are filled with neon at a pressure of about 70 Torr. Three tubes are installed

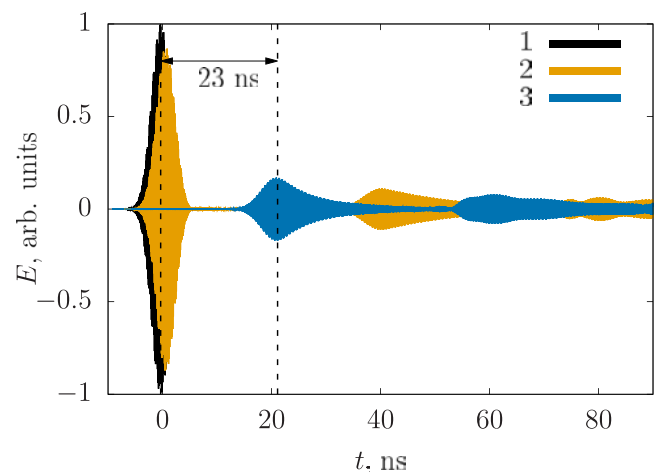


FIG. 3. Simulated electric field strength for the incident (1), reflected (2), and transmitted (3) waves.

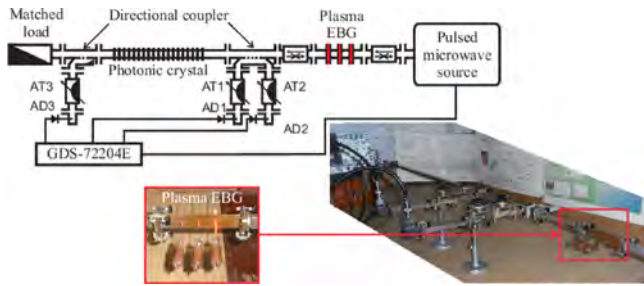


FIG. 4. The experimental layout and the setup photo.

perpendicularly to the wider wall of the waveguide at 30 mm distance from each other (see Fig. 4, inset at the bottom). When the discharges with electron density exceeding  $10^{14} \text{ cm}^{-3}$  are initiated in the tubes by microwave breakdown, the plasma electromagnetic crystal, whose stop band central frequency is about 9.15 GHz, is formed.<sup>25</sup> Suppression at this frequency exceeds 30 dB. This leads to a sharp change of waveguide section transmittance for frequency 9.15 GHz and provides shortening of the incident microwave pulse (truncation of the incident pulse).<sup>26</sup> The duration of the microwave pulse that passed through the plasma EBG crystal is defined by time of electron concentration growth to values exceeding  $10^{14} \text{ cm}^{-3}$ . This duration is defined by the power of the initial microwave pulse and its rise-time.

Figure 5 demonstrates the microwave pulses incident on and passed through the plasma EBG structure. The duration of the microwave pulse passed through it is about 4 ns.

The microwave pulse shortened and reduced in amplitude by the plasma EBG structure is guided to the photonic crystal [see Figs. 4 and 6(a)] by a directional coupler. Part of the incident to the photonic crystal microwave power is guided by an additional coupler, attenuator AT1, and waveguide-to-coaxial transition AD1 to a microwave diode and detected by an oscilloscope GDS-72204E (200 MHz, 1 Gigasample/s). Reflected and transmitted pulses are similarly detected by the same oscilloscope via channels AT2-AD2-microwave diode and AT3-AD3-microwave diode, respectively. The oscilloscope is triggered by a sync pulse from the microwave source. To ensure equity of measuring arms, the

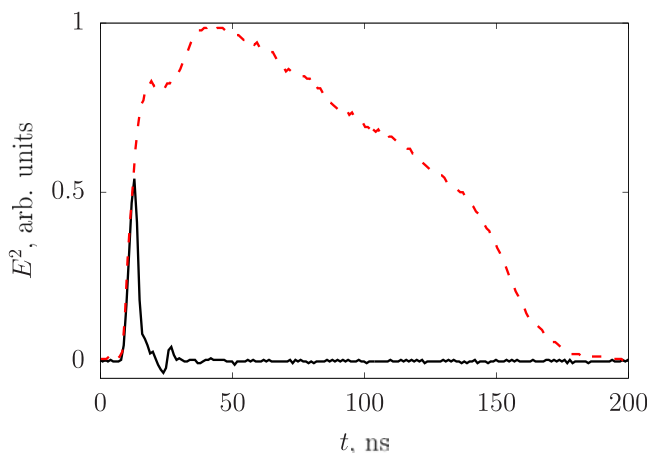
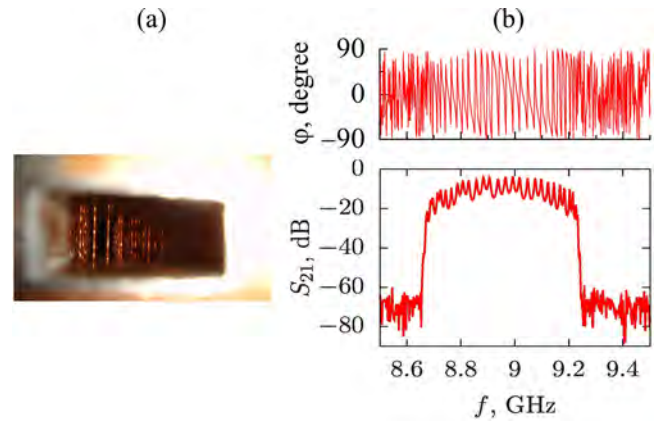


FIG. 5. Microwave pulses incident on the plasma EBG structure (dashed line) and passed through it (solid line).

FIG. 6. Photonic crystal photo (a) and (b) measured phase  $\varphi = \arg(S_{21})$  and  $S_{21}$  dependence on frequency.

layout was preliminary tested with the empty waveguide (without a periodic structure of copper rods inside) replacing the photonic crystal of the equal length.

The photonic crystal spectrum measured by a vector analyzer Anritsu MS4645B [see Fig. 6(b)] includes a single pass band in the range 8.65–9.25 GHz (X-band). It is similar to the calculated photonic crystal spectrum, which is shown in Fig. 1(b).

### III. RESULTS AND DISCUSSION

The microwave pulse transmitted through the photonic crystal is normalized to the power of the incident pulse and compared with that obtained in simulation. The detected envelope of the microwave pulse incident on the photonic crystal is shown in Fig. 7 by a (line + symbols) curve. The envelope shaded area in Fig. 7 shows squared electric field strength  $E^2$  for the pulse used in simulation. The microwave pulse transmitted through the photonic crystal, which is detected in the experiment, is shown in Fig. 8 by a (line + symbols) curve; simulation results are presented therein by the shaded area.

Comparison of experimentally obtained and simulated pulse envelopes in Fig. 8 demonstrates good agreement in shapes of peaks and their amplitudes. The amplitude of the

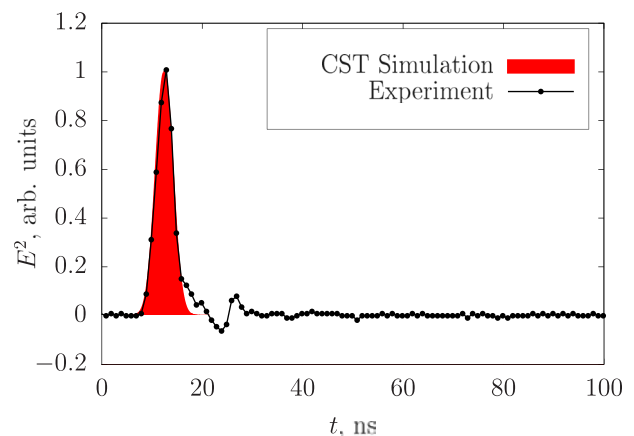


FIG. 7. The envelope of the microwave pulse incident on the photonic crystal: experiment (line + symbols curve) and simulation (shaded area).

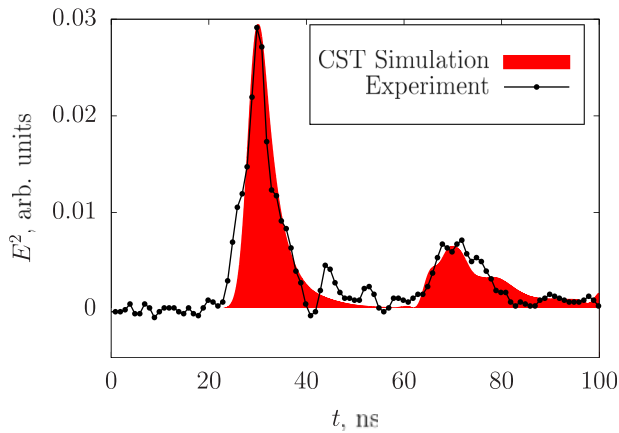


FIG. 8. The microwave signal transmitted through the photonic crystal: experiment (line + symbols curve) and simulation (shaded area).

transmitted pulse is observed to be 30 times smaller as compared to the amplitude of the incident pulse. The observed delay time is  $\tau \approx 23$  ns that is also in good agreement with simulation results. In our experiments, the time delay measurement deviation was  $\pm 1$  ns (about 5%). The pulse group velocity  $v_{gr}$  in the photonic crystal is  $v_{gr} = L_{cr}/\tau \approx 3.2 \times 10^7$  m/s  $\approx 0.11c$ , where  $c$  is the speed of light in vacuum. The similar values of group velocity (about  $c/20$ ) were reported<sup>13,14</sup> for optical pulses in photonic crystals. Both detected and simulated transmitted pulses Fig. 8 contain the additional peak delayed for about  $2\tau \approx 46$  ns with respect to the first one.

#### IV. CONCLUSION

The optimal conditions to observe pulse delay due to Bragg diffraction in the photonic crystal are simulated and experimentally realized for the microwave pulse, whose central frequency is 9.15 GHz. The photonic crystal is designed as a spatially periodic structure built of copper rods inside a WR90/R100 waveguide. Measured and simulated time delay amounts to  $\tau \approx 23$  ns and corresponds to the group velocity value  $v_{gr} \approx 0.11c$ . The simulated transmitted and reflected pulses are shown to have oscillations of intensity, which at the incident pulse duration from 5 to 20 ns are distinctly separated with the time distance between maxima  $2\tau \approx 46$  ns. The similar oscillations of the intensity for the transmitted

pulse are detected in the experiment in full accordance with the simulation results. The obtained results can be applied in high-speed information transmission systems, which use periodic crystal-like structures to control propagation of radiation.

- <sup>1</sup>L. Brillouin, *Wave Propagation and Group Velocity* (Academic Press, New York, 1960).
- <sup>2</sup>E. B. Aleksandrov and V. S. Zapasskii, *Phys. Usp.* **49**, 1067–1075 (2006).
- <sup>3</sup>F. N. Chukhovskii and E. Forster, *Acta Cryst.* **A51**, 668–672 (1995).
- <sup>4</sup>V. G. Baryshevsky, *Izv. Akad. Nauk BSSR, Ser. Fiz.-Mat.* **5**, 109112 (1989).
- <sup>5</sup>V. G. Baryshevsky, e-print [arXiv:physics/9906022](https://arxiv.org/abs/physics/9906022).
- <sup>6</sup>J. M. H. Sheppard, R. W. Lee, and J. S. Warka, *Proc. SPIE* **4500**, 101–112 (2001).
- <sup>7</sup>J. S. Wark, A. M. Allen, P. C. Ansbro *et al.*, *Proc. SPIE* **4143**, 26–37 (2001).
- <sup>8</sup>S. D. Shastri, P. Zambianchi, and D. M. Mills, *J. Synchrotron Radiat.* **8**, 1131–1135 (2001).
- <sup>9</sup>V. V. Voronin, E. G. Lapin, S. Y. Semenikhin, and V. V. Fedorov, *JETP Lett.* **71**(2), 76–79 (2000).
- <sup>10</sup>T. Baba, *Nat. Photonics* **2**, 465–473 (2008).
- <sup>11</sup>D. V. Novitsky, *Phys. Rev. A* **84**(5), 053857 (2011).
- <sup>12</sup>D. V. Novitsky, *J. Opt.* **15**(3), 035206 (2013).
- <sup>13</sup>C.-Y. Lin, H. Subbaraman, A. Hosseini, A. X. Wang, L. Zhu, and R. T. Chen, *Appl. Phys. Lett.* **101**(5), 051101–051104 (2012).
- <sup>14</sup>X. Zhang, C.-J. Chung, A. Hosseini, H. Subbaraman, J. Luo, A. K.-Y. Jen, R. L. Nelson, C. Y.-C. Lee, and R. T. Chen, *J. Lightwave Technol.* **34**(12), 2941–2951 (2016).
- <sup>15</sup>H. Gersen, T. J. Karle, R. J. P. Engelen, W. Bogaerts, J. P. Korterik, N. F. van Hulst, T. F. Krauss, and L. Kuipers, *Phys. Rev. Lett.* **94**(7), 073903 (2005).
- <sup>16</sup>A. Silva, F. Monticone, G. Castaldi, V. Galdi, A. Ala, and N. Engheta, *Science* **343**, 160–163 (2014).
- <sup>17</sup>N. V. Golovastikov, D. A. Bykov, and L. L. Doskolovich, *Opt. Lett.* **40**, 3492 (2015).
- <sup>18</sup>Y. Jiang, B. Howley, Z. Shi, Q. Zhou, R. T. Chen, M. Y. Chen, G. Brost, and C. Lee, *IEEE Photonics Technol. Lett.* **17**(1), 187–189 (2005).
- <sup>19</sup>J.-M. Brosi, J. Leuthold, and W. Freude, *J. Lightwave Technol.* **25**(9), 2502–2510 (2007).
- <sup>20</sup>J. D. Joannopoulos, S. G. Johnson, J. N. Winn, and R. D. Meade, *Photonic Crystals: Molding the Flow of Light* (Princeton University Press, 2008).
- <sup>21</sup>V. G. Baryshevsky and A. A. Gurinovich, e-print [arXiv:1101.4162](https://arxiv.org/abs/1101.4162).
- <sup>22</sup>S. V. Anishchenko, V. G. Baryshevsky, and A. A. Gurinovich, *Nucl. Instrum. Methods B* **293**, 35–41 (2012).
- <sup>23</sup>S. V. Anishchenko, V. G. Baryshevsky, and A. A. Gurinovich, *J. Nanophotonics* **6**, 061714 (2012).
- <sup>24</sup>See [www.cst.com/products/cstmws](http://www.cst.com/products/cstmws) for CST, Computer Simulation Technology.
- <sup>25</sup>V. I. Arkhipenko, T. Callegari, L. V. Simonchik, J. Sokoloff, and M. S. Usachonak, *Appl. Phys.* **116**, 123302 (2014).
- <sup>26</sup>L. V. Simonchik and M. S. Usachonak, Russian Federation patent 2520374 (2013).